J Comp Physiol A (2008) 194:255–265
DOI 10.1007/s00359-007-0303-1

ORIGINAL PAPER

# Influence of sound pressure level on the processing of amplitude modulations by auditory neurons of the locust

**Gerroth Weschke · Bernhard Ronacher**

Received: 2 November 2007 / Revised: 23 November 2007 / Accepted: 23 November 2007 / Published online: 12 December 2007


**Abstract** Typical features of natural sounds are amplitude changes at different time scales. In many species, amplitude modulations constitute decisive cues to recognize communication signals. Since these signals should be recognizable over a broad intensity range, we investigated how the encoding of amplitude modulations by auditory neurons depends on sound pressure level. Identified neurons that represent different processing stages in the locusts' auditory pathway were stimulated with sinusoidal modulations of a broad band noise carrier, at different intensities, and characteristic parameters of modulation transfer functions (MTFs) were determined. The corner frequencies of temporal MTFs turned out to be independent of intensity for all neurons except one. Furthermore, for none of the neurons investigated corner frequencies were significantly correlated with spike rate, indicating a remarkable intensity invariance of the upper limits of temporal resolution. The shape of the tMTFs changed with increasing intensity from a low-pass to a band-pass for receptors and local neurons, while no consistent change was observed for ascending neurons. The best modulation frequency depended on intensity and spike rate, especially for receptors and local neurons. Remarkably, the adaptation state of some neurons turned out to be independent of the spike rate during the modulation part of the stimulus.

**Keywords** Modulation transfer functions · Temporal resolution · Intensity invariance · Adaptation · Grasshoppers

G. Weschke · B. Ronacher (✉)
Institut für Biologie der Humboldt-Universität zu Berlin, Abt. Verhaltensphysiologie, Invalidenstr. 43, 10099 Berlin, Germany
e-mail: bernhard.ronacher@rz.hu-berlin.de

**Abbreviations**

| | |
|---|---|
| AM | Amplitude modulation |
| AN | Ascending neuron |
| BMF | Best modulation frequency |
| rMTF, tMTF | (Rate and temporal) modulation transfer function |
| SAM | Sinusoidal amplitude modulation |
| SPL | Sound pressure level |

## Introduction

Amplitude modulations (AM) are a characteristic feature of acoustic communication signals across different taxa (Michelsen 1985; Kroodsma and Miller 1996; Gerhardt and Huber 2002). In many species, including our own, rapid fluctuations in the sound envelope convey important information, which has to be deciphered by the receiver on time scales of a few milliseconds. Hence, the ability to resolve AMs with adequate temporal resolution and the ability to focus upon the relevant frequency range of AMs are the fundamental tasks of auditory systems (Joris et al. 2004). Auditory receptors generally do phase-lock their spike responses to the signal envelope, up to high modulation frequencies, while their spike rates do not depend on AM frequency. Since receptor neurons obviously code the AM in the periodicity of their discharges, the precision of spike timing will be crucial for the representation of AMs at this most peripheral processing level. At more central processing stages, however, the phase locking is gradually substituted by rate-based coding strategies (see e.g. Rose and Capranica 1985; Grothe 1994; Rhode and Geeenberg 1994; Alder and Rose 2000). In mammals, auditory neurons were described whose firing rates are sharply tuned to

certain AM frequencies, and there seems to exist a bank of such AM filters, potentially enabling to analyse the AM frequency composition of acoustic signals (Langner 1992; Joris et al. 2004). The processing of AMs is of particular relevance for animals that have ears with poor resolution of carrier frequencies, as is the case in many insects (Stumpner and von Helversen, 2001; Hennig et al. 2004). Indeed, the acoustic communication signals of many insects are characterized by a lack of tonality but a rich repertoire of periodic AM patterns—which necessitates a corresponding receiver system capable of resolving and detecting the species-specific AM patterns.

Communication signals should be recognizable over a broad intensity range. This study therefore focuses upon the impact of sound pressure level (SPL) on the encoding of AMs by auditory neurons. A signal's average SPL does affect spike rates and, indirectly, also the variability of spiking responses, two factors that likely delimit the temporal resolution of auditory neurons (Rhode and Greenberg 1994; Krishna and Semple 2000; Vogel et al. 2005, Vogel and Ronacher 2007; Wohlgemuth and Ronacher 2007). Hence, for a correct interpretation of acoustic signals by the central nervous system it is necessary to disambiguate the influences of modulation frequency and sound intensity on neuronal responses. A crucial question in this context is how intensity invariant are the temporal processing properties of auditory neurons?

We investigated this problem in auditory neurons located within the metathoracic ganglion of grasshoppers, which is a well-established model for the processing of acoustic patterns (e.g. Römer and Marquart 1984; Stumpner et al. 1991; Machens et al. 2001). This auditory pathway is hierarchically organized, and consists of three consecutive stages of processing: receptor neurons, local interneurons (LN), and ascending interneurons (AN), which transmit the pre-processed information to higher centres located in the animal's brain (Römer and Marquart, 1984; Ronacher et al. 1986; Stumpner et al. 1991). Interestingly, the variability of spike trains, measured with unmodulated stimuli, increases towards more central processing levels, from receptors to local neurons, and further to ascending neurons (Vogel et al. 2005). This increase of variability at more central processing levels is at least partly due to a parallel reduction in maximum spike rates. It should be mentioned, however, that the precision of spiking responses depends as well on other factors than the mean signal level, in particular the depth and steepness of amplitude rise of AMs (Machens et al. 2001; Rokem et al. 2006).

We used modulation transfer functions (MTF) to investigate how the temporal processing properties of auditory neurons may change with sound intensity. MTFs are a standard paradigm to characterize the temporal resolution and the processing of AM by auditory systems (Rhode and Greenberg 1994; Krishna and Semple 2000; Prinz and Ronacher 2002; Joris et al. 2004). Our aim was to investigate how stable MTF properties are against changes in SPL, and the concomitant changes in spike rates and spike timing precision, and whether there exist differences between processing levels.

## Material and methods

### Animals and electrophysiology

The animals used in all experiments were adult male and female locusts (*Locusta migratoria*), which were obtained from a local supplier and held at room temperature (22–25°C). After removal of head, legs, and wings, animals were waxed with their dorsal side up onto a Peltier element (3 cm × 1.5 cm) attached to a free-standing holder. The thorax was opened dorsally and the metathoracic ganglion was exposed and stabilized by a small NiCr platform. The whole torso was filled with locust Ringer solution (Pearson and Robertson 1981). The temperature of the preparation was adjusted to 30°C by means of the Peltier element and a digital thermo sensor positioned in the abdomen.

Intracellular recordings were obtained from auditory receptors, local and ascending interneurons in the frontal auditory neuropil of the metathoracic ganglion. We used standard electrophysiological techniques and equipment (for details see Krahe and Ronacher 1993; Vogel et al. 2005). After amplifying the intracellular voltage signal (Bramp-01R, NPI), it was fed through a 10-kHz low-pass filter. The tips of glass (Harvard Apparatus Ltd.) or quartz microelectrodes (Sutter instruments) were filled with a 3–5% solution of Lucifer Yellow (Aldrich) in 0.5 M LiCl. This dye was injected after completion of the physiological recording by applying hyperpolarizing current. At the end of an experiment, the thoracic ganglia were fixed in 4% paraformaldehyde, dehydrated and cleared in methylsalicylate. Stained cells were identified under a fluorescence microscope on the basis of their characteristic morphology (terminology after Römer and Marquart 1984; Stumpner and Ronacher 1991). Locusts can be used as models for other grasshoppers, since auditory neurons in different grasshoppers exhibit high similarity, not only in their morphology but also in their physiological responses (Stumpner 1988; Wohlgemuth et al. 2007).

### Acoustic stimulation

Experiments were performed in a Faraday cage (93 × 67 × 79 cm) lined with reflection attenuating

pyramidal foam. The preparation was acoustically stimulated via two loudspeakers situated laterally at a distance of 35 cm. Sound intensity was calibrated using a Brüel and Kjær microphone (1/2 in) positioned at the place of the animal and a Brüel and Kjær measuring amplifier (type 2231). Intensities are given in dB re $2 \times 10^{-5}$ N/m$^2$ (dB SPL). All stimuli were stored digitally and displayed by custom software (Labview, National Instruments) using a 100 kHz D/A-converter (PCI-MIO-16E-4, National Instruments).

Two different stimulus types were applied: first, in order to obtain an intensity response curve, unmodulated pulses of 100 ms duration (2 ms rise and fall times) filled with broad-band noise (bandwidth 0.5–30 kHz) were presented at intensities ranging from 35 to 89 dB in 6 dB steps. At each intensity, the stimuli were repeated three times. Second, in order to obtain MTFs we used sinusoidally amplitude modulated (SAM) stimuli with 100% modulation depth (see Krishna and Semple 2000). SAM-stimuli were constructed by multiplying a broad-band noise carrier (bandwidth 0.5–30 kHz) with a sine of defined modulation frequency. The modulation frequencies used were 5, 10, 20, 40, 83.3, 125, 166.6, 250, 500, and 1,000 Hz. Each SAM stimulus was preceded by a 200-ms-segment of unmodulated noise (an adaptation pulse), followed by a 1-s segment of constant modulation frequency and another segment of 200 ms of unmodulated noise (which served as control pulse for the level of adaptation); adaptation and control pulse had the same peak height as the SAM part of the stimulus (see Fig. 1). Each SAM-stimulus was repeated six times, and modulation frequencies were presented in a pseudorandom order. All stimuli were generated in the Labview programming environment (National Instruments).

As soon as an auditory neuron was impaled, as a first step an intensity response curve was determined online. The intensities at which MTFs were measured were chosen according to these curves: the first MTF was obtained at an intensity that evoked maximum spike rates. For the second MTF, a lower intensity was used at which the cell fired with roughly 50% of its maximal firing rate. If the recording was stable enough, a second intensity response curve based on five repetitions per intensity was determined as a control, and additional MTFs at further intensities were obtained if possible.

## Data analysis

Spiking responses were digitized at 20 kHz (A/D converter, PCI-MIO-16E-4, National Instruments). Spike times were determined with 0.05 ms precision from the digitized recordings by means of a voltage threshold criterion. The resulting spike trains represented the basis for all subsequent analyses. MTFs based on rate (rMTF) were determined by plotting the spike rate averaged over the six repetitions of the SAM part of the stimulus against the modulation frequency. A deviation from an all pass filter was recognized, if spike rates of at least two consecutive modulation frequencies deviated by at least 40% from the average spike rate of that cell (Franz 2004). This rather conservative criterion was chosen to reduce the influence of obviously random spike rate fluctuations, as some rMTFs had a jagged appearance (Fig. 2; cf. also Hall and Feng 1991).

In order to obtain vector strength-based modulation transfer functions (tMTF), period histograms were generated from the SAM part of the stimulus. Each period histogram was divided in 30 bins; i.e. bins cover different absolute time scales depending on the modulation frequency. From these period histograms the vector strength was calculated using formula (1):

$$\mathrm{VS} = \sqrt{\left(\frac{1}{n}\sum_{i=1}^{n}\cos\alpha_i\right)^2 + \left(\frac{1}{n}\sum_{i=1}^{n}\sin\alpha_i\right)^2} \qquad (1)$$

with $\alpha_i$ denoting spike times expressed as the phase of stimulus. Rayleigh's $\mathbf{z}$ was calculated to control for the significance of phase locking. A value of $\mathbf{z} = 3$, which corresponds to a 5% significance level, was chosen as threshold (Gleich and Klump 1995; Prinz and Ronacher 2002). Only at high modulation frequencies (250 Hz or higher) Rayleigh's $\mathbf{z}$ regularly fell below this threshold criterion. Therefore, phase locking was significant in almost all tMTFs up to 166.6 Hz. Following Hall and Feng (1991) and Feng et al. (1991), corner frequencies of tMTFs were determined as the modulation frequency where the vector strength dropped to 50% of its maximal value, a value which normally fell into the steepest part of the tMTF curves. This is a conservative criterion, which was chosen to reduce the effect of chance fluctuations in the tMTF curves.

For statistical analysis Wilcoxon's matched pairs test was used to compare high against low intensity data (Sachs 1999). If more than two MTFs could be measured in one cell, the MTF obtained at the highest and the lowest intensity was used for the test. Data are presented separately for four groups of neuron types, depending on the processing level, and on how often recordings from one cell type were possible. These four groups were receptors together with SN1, TN1, BSN1, and the ascending neurons (AN). Although the ascending neurons encompass different types with partly different response properties (Römer and Marquart 1984, Stumpner and Ronacher 1991), we decided not to split up the data of ascending neurons in more groups since too few specimens of each type were recorded. However, some

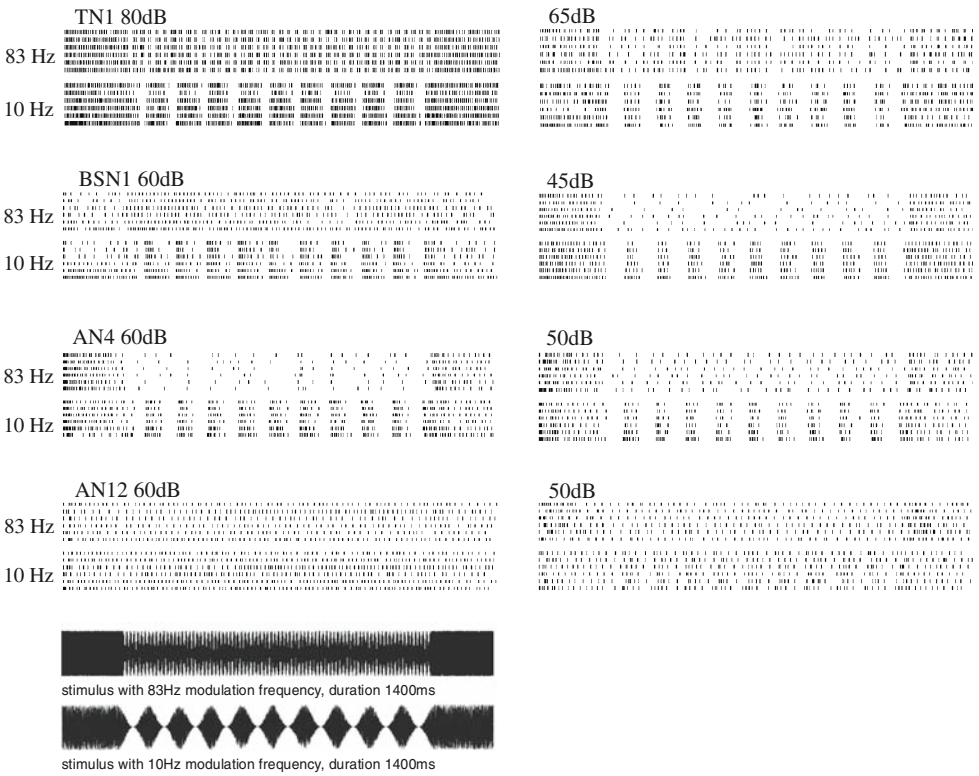


**Fig. 1** Raster plots of spike trains from four neuron types, at different intensities and modulation frequencies (10 and 83 Hz); on the *bottom* also shown are the corresponding stimuli, composed of an adaptation block, the SAM part, and a control block stimulus

general coding principles can be derived from such a grouping as well (see also Vogel et al. 2005; Vogel and Ronacher 2007; Wohlgemuth and Ronacher 2007).

Multiple MTFs were recorded from a total of 43 auditory neurons [7 receptor neurons, all of the low-frequency type, 24 local neurons (1 SN1, 16 TN1, 7 BSN1), and 12 AN (one AN1, AN2, AN4; and three specimens of AN3, AN11, and AN12), terminology according to Römer and Marquart 1984; Stumpner and Ronacher 1991).

## Results

The steps of data evaluation are demonstrated in Figs. 1 and 2, for four neuron types: TN1, which is a neuron with primary-like response characteristic; BSN1, a local neuron that is an important distributor of auditory information to other neurons (Boyan, 1992) and has its main arborizations in the metathoracic ganglion but extends an axon to the mesothoracic ganglion; AN4 and AN12 belong to the class of ascending neurons, which transmit the pre-processed information to the animal's brain. Figure 1 shows the raster plots of spike trains obtained at two modulations frequencies, 10 and 83 Hz, and two different intensities. These plots give an impression of a neuron's ability to phase lock to the stimulus envelope, and also of the trial-to trial variability of spike responses. Both factors will influence properties of the MTF, in particular up to which frequency a neuron may resolve AMs. On the basis of this type of data, the rMTF and tMTF are shown in Fig. 2b, c, in the middle and right columns, respectively. The left hand column presents intensity response curves obtained with 100 ms block stimuli (see "Materials and methods" section), which were used to adjust the sound intensities for the MTF program. Note, however, that in general the spike rates found in the MTF were lower than those in the intensity response curves. This is partly due to the reduced energy in the SAM part of the stimuli compared to the block stimuli, but probably also to adaptation, which was less intense for the short stimuli used to determine these curves (see also below).

### Temporal modulations transfer functions

In the following, we focus first on the temporal MTFs, based on vector strength. Several parameters can be used to describe characteristic properties of tMTF. An important measure is the *corner frequency*, which indicates the modulation frequency limit up to which a cell is able to lock its spike response to the stimulus envelope. A second parameter is the *maximum vector strength*, which indicates whether the phase locking of spikes is exact or rather sloppy. A third feature is the *best modulation frequency* (BMF), i.e. the modulation frequency at which the most precise phase locking of spikes occurs (see Rhode and Greenberg 1994, for definition). These three parameters

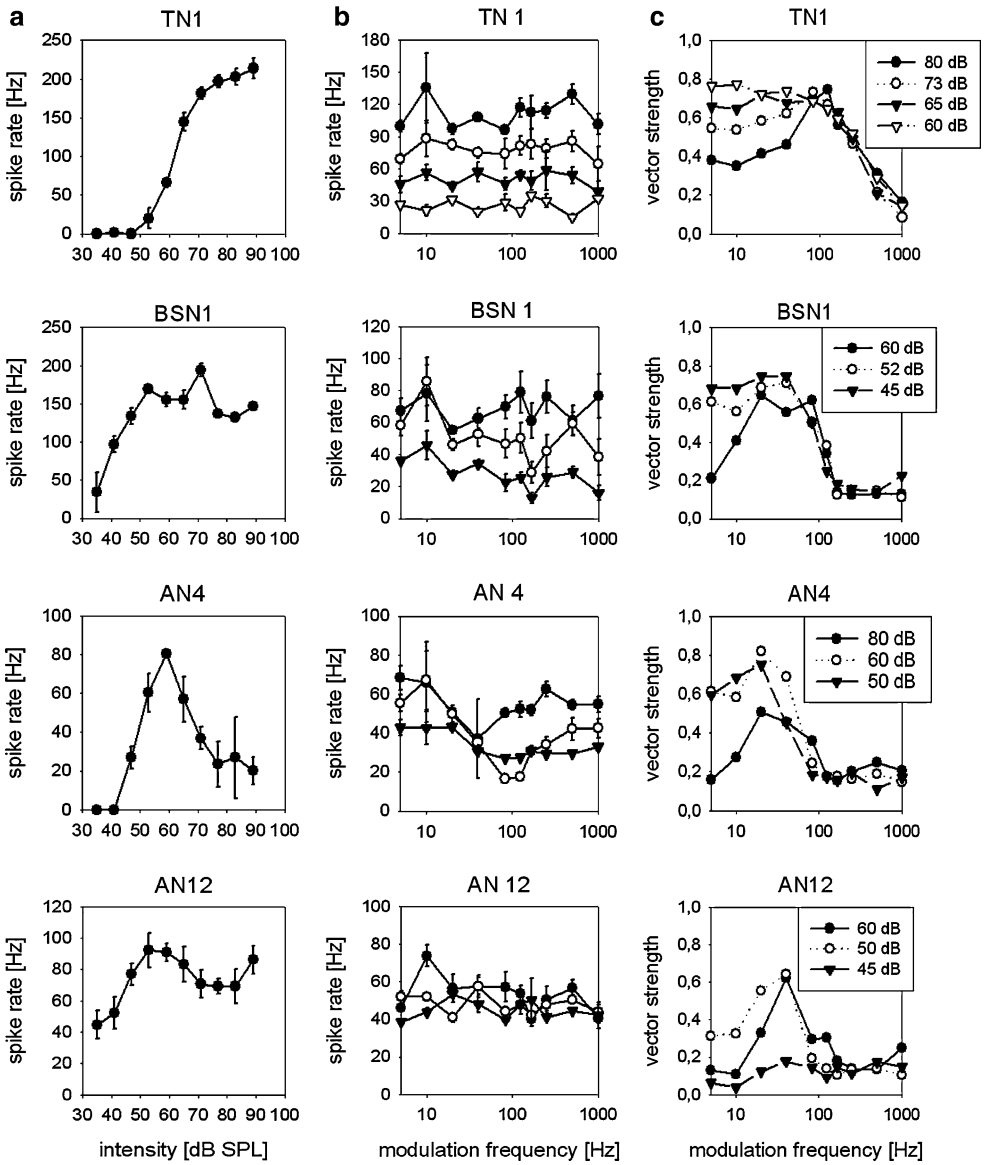


**Fig. 2** Intensity response curves (**a**), rate modulation transfer functions (**b**) and temporal MTFs (**c**) for the same neurons as in Fig. 1. Intensities used for the MTFs are depicted in the *insets* in **c**. Further explanations in text

will be analysed and compared in the following for the different processing levels. Furthermore, we present an evaluation, which compares the tMTF according to their low- or band-pass properties.

### *The upper limit of temporal resolution is largely independent of sound intensity and spike rate*

We determined corner frequencies to describe the upper limits of temporal resolution, i.e. the modulation frequency at which a neuron ceases to phase lock its spikes to the stimulus envelope. Figure 3a shows the corner frequencies of receptors (and one SN1), which were mostly above 100, up to 350 Hz, but showed no consistent dependence on intensity (values obtained from a cell at different intensities are connected by a line, in order to visualize possible trends). The 16 TN1 neurons exhibited even higher corner frequencies, up to 500 Hz. In contrast to receptors, for this neuron type a significant trend existed that the corner frequency decreased at high intensities (most lines in Fig. 3b have a negative slope). The corner frequencies of BSN1 were restricted to the range between 100 and 200 Hz, but showed no significant correlation with intensity (Fig. 3c). Compared to the local neurons, the corner frequencies of ascending neurons were shifted towards lower frequencies, mostly between 50 and 150 Hz—which is in accord with published data (Wohlgemuth and Ronacher 2007)—and again no general trend with intensity was visible (Fig. 3d).

In order to explore possible indirect influences of sound intensity, via different spike rates, we calculated mean spike rates for all data of Fig. 3 and plotted the corner frequencies against spike rates (Fig. 4). Remarkably, in no case there was

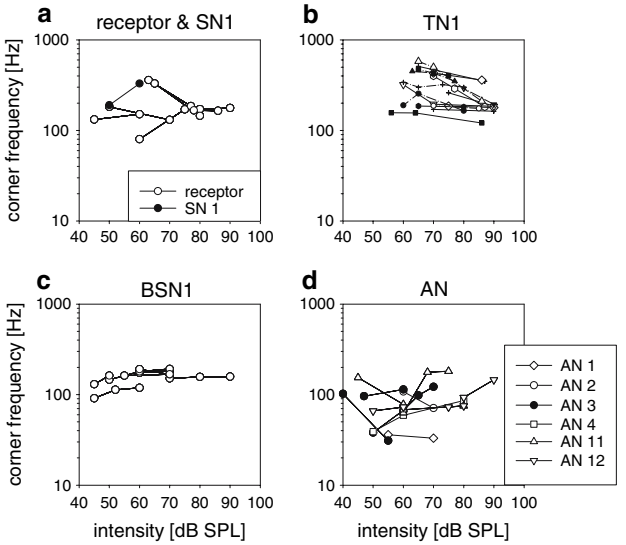


**Fig. 3** Corner frequencies derived from the tMTF at different intensities, for different classes of neurons. Data obtained from one specimen at different intensities are connected by *lines*, to visualize trends. A significant trend could be confirmed only for the large sample of TN1 ($P < 0.001$, Wilcoxon matched pairs test, see "Material and methods" for data evaluation). **a** Data of 7 receptors and 1 SN1; **b** data of 16 TN1; **c** data of 7 BSN1; **d** data of AN1, AN2, 3 AN3, AN4, 3 AN11, and 3 AN12

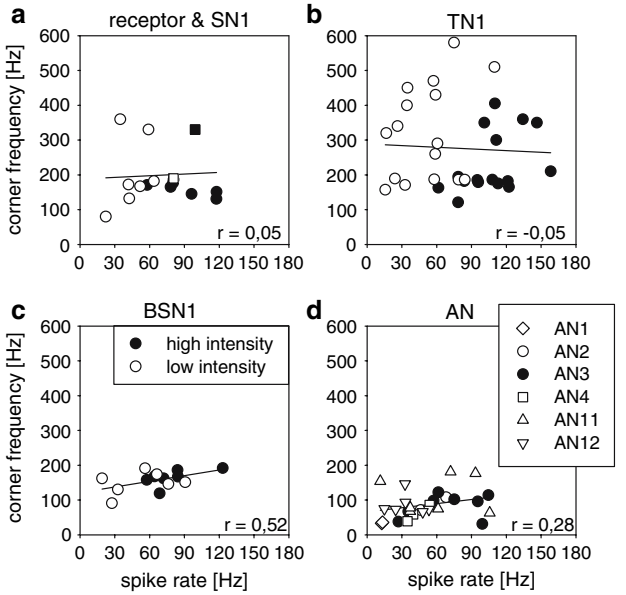


**Fig. 4** Corner frequencies plotted against mean spike rates. Spike rates are given as mean rate averaged over all frequencies. In most cases averaging was no problem since almost all neurons exhibited allpass characteristics in their rMTF (see TN1, BSN1 and AN12 in Fig. 2; for a few exceptions see Fig. 8 and text). Data of same neurons as in Fig. 3. *Open* and *filled symbols* in **a-c** indicate data from low and high intensities, respectively

a significant correlation observed, not even for TN1, of which 16 specimens were recorded. For BSN1 and the ascending neurons there was a weak but not significant trend that higher spike rates resulted in higher corner frequencies.

### *The shape of the tMTF depends on intensity*

The tMTFs of all neurons exhibited low-pass or band-pass characteristics (Fig. 2, right column)—so far we found no neuron with high-pass properties in its tMTF. For receptor neurons and local neurons it depended on intensity which type of MTF was found. With increasing SPL the tMTF of most neurons underwent a change from a low-pass to a distinct band-pass characteristic (Fig. 2, right column). This behaviour can be understood when looking at the 10 Hz data of TN1 or BSN1 in Fig. 1. At the lower intensity, spikes were clustered around the peaks of the sinusoidal AM, while at the higher intensity, spikes occupy a larger proportion of the stimulus period, thus leading to a reduced vector strength. In order to present a compilation of all recorded cells, we calculated the difference between the maximum vector strength and the vector strength at a modulation frequency of 10 Hz for each tMTF. A low-pass curve will yield a zero or only a minor difference while a more pronounced band-pass is characterized by an increasing difference (compare Fig. 2). Figure 5 shows this evaluation for every recorded neuron; data of one specimen at different intensities are connected by a line. All receptor neurons and the local neurons with primary-like responses, SN1 and TN1, showed this intensity dependent change from low-pass to band pass very clearly (Wilcoxon, $P < 0.01$ and 0.001); for the other local neuron BSN1 a similar but not significant tendency was observed. For the ascending neurons there was no uniform trend. The tMTF of some neurons changed from band-pass to low-pass at higher intensity, some exhibited the reverse change, while still others showed no change in the shape of tMTF.

There are large differences between the curves of individual receptors in Fig. 5a. At, for example, 65 dB some specimens exhibit a low pass, others a clear band pass characteristic. These differences probably result from large variations in threshold typical for receptors tuned to low frequencies (Römer 1976). The data of TN1 show a tighter clustering along the SPL axis, which corresponds to the notion that TN1 is driven by a population of less sensitive receptors only (Römer and Marquart 1984; Stumpner 1988). In general, however, a direct comparison of thresholds between individual specimens of different neuron types is not feasible with our approach, since in most cases only one neuron per animal was recorded from, and therefore interindividual differences in general sensitivity cannot be excluded.

Another characteristic of tMTFs is the maximum vector strength, which reflects the precision of spiking responses.

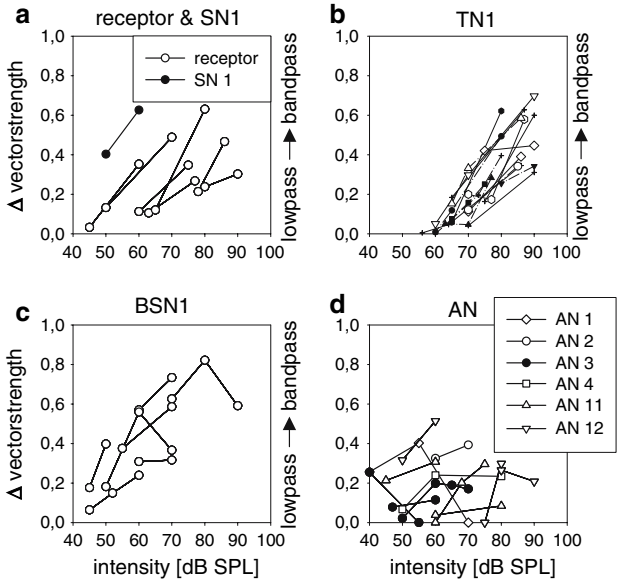


**Fig. 5** Intensity-dependent changes of tMTF shape. To compare low-pass and band-pass properties of the tMTF, we calculated for each neuron the difference between the maximum vector strength and the vector strength at 10 Hz modulation frequency. An increasing difference indicates a shift form low-pass to band-pass behaviour (see *right ordinate*). Data obtained from one cell at different intensities are connected by *lines*. Further explanations in text

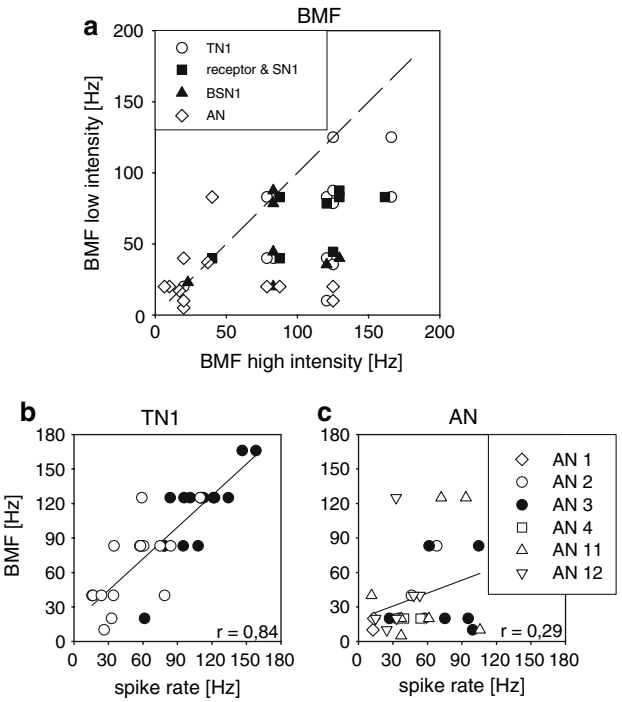


**Fig. 6** Dependence of the best modulation frequency (BMF) on intensity (**a**) and spike rate (**b**, **c**). In **b**, **c**, regression lines are shown (**b**: $P < 0.001$; **c** n.s.). The BMFs of receptors and BSN1 depended in a very similar way on spike rate, as those of TN1 ($r = 0.70$ and $r = 0.68$; data not shown). *Filled* and *open symbols* in **b** indicate high and low intensities, respectively

For most neurons, the maximum vector strength did depend only marginally and not systematically on intensity (Wilcoxon, $P > 0.05$; see e.g. TN1, BSN1 in Fig. 2). For receptors and local interneurons, the mean values of maximum vector strength were highly similar (receptors $0.74 \pm 0.11$; TN1 $0.75 \pm 0.05$; BSN1 $0.78 \pm 0.1$; mean $\pm$ SD). Taken across all ascending neurons, a smaller mean value and a much larger variation were observed ($0.58 \pm 0.25$, range 0.25–0.93). However, for the ascending neurons again no consistent dependence of max vector strength on intensity was visible (not shown). An intensity rise could induce an increase as well as a decrease in peak vector strength (see AN4 in Fig. 2 as an example for the latter).

While the value of maximum vector strength did not depend on intensity, its position on the frequency axis—the best modulation frequency, BMF—did, for the majority of cells. Although this effect is not evident in examples of Fig. 2, an increase of sound intensity induced a shift towards a higher BMF for the majority of neurons (Fig. 6 a). With the exception of the AN-neurons, the BMF did correlate also with the mean spike rate (Fig. 6b, c).

## Rate MTFs

The rate MTFs yielded often rather jagged curves (compare Fig. 2). We therefore used a rather conservative criterion to classify MTFs, a drop of at least 40% compared to the average spike rate (see "Materials and methods" section). Using this definition, rate MTFs of 37 of 43 (86%) neurons were all-pass, and showed no consistent change of their characteristic with intensity, except for a shift along the spike count axis (Fig. 2). However, there were a few exceptions of this generalization; one of them was the AN4 neuron (Fig. 2, middle column, 60 dB). As also reported by Franz (2004), this neuron shows a band stop behaviour: AM frequencies around 100 Hz lead to a drastic reduction in spike rates, to a third or even less (see also raster plot at 60 dB, in Fig. 1), while spiking is restored at higher MFs (Fig. 2, open circles). This particular response of the AN4 is due to a leading inhibitory postsynaptic potential (IPSP), which is triggered by a steep amplitude rise after a period of quiet, and effectively suppresses spiking activity (Ronacher and Stumpner 1988; Stumpner et al. 1991; Franz and Ronacher 2002). At low frequencies of a sinusoidal AM as used here, the slope of the rise is too shallow to trigger the IPSP, while at frequencies above $\sim$250 Hz the period of silence in the troughs becomes too small, and the signal appears no longer different from an uninterrupted one (Franz 2004). This band stop response was, however, reduced at low and also at very high intensities (Fig. 2). Among the local neurons, three BSN1 specimens exhibited a low-pass

characteristic, at least at low intensities, while another BSN1 showed a band-pass rMTF (see below). Within our sample of ascending neurons only the rMTF of AN4 and of one AN3 (weak band-stop) deviated markedly from the all-pass type.

## Adaptation effects

Different SPLs of signals do not only affect a neuron's spike rate but also its adaptation time constants (Benda et al. 2001), which in turn may affect features of temporal processing. Our stimuli were designed as to bring the neurons into an adapted state by means of an unmodulated 200 ms pulse of noise which preceded each SAM stimulus (see Figs. 1, 7). After the SAM part, there followed another 200 ms pulse, which allowed to check for possible adaptation changes induced by different modulation frequencies (see Fig. 8). Figure 7 compares the mean spike rates observed during the first, adaptation pulse (abscissa), and the rates during the second, control pulse (ordinate). Spike rates during the control pulse were in general reduced, in particular at higher spike rates. However, for receptors and local neurons, the extent of this reduction was modest, rarely exceeding 30%. Only in some ascending neurons the spike rates decreased by 50% and more. Note that due to the bell-shaped intensity–response curves of some neurons (Fig. 2), spike rates at high intensity can be smaller than at the low intensity. In the graphs of Fig. 7 no distinction was performed according to the modulation frequencies. This appeared to be not necessary in view of the—mostly uniform—all-pass shape of the rMTFs. However, in a few cases in which the rMTF clearly deviated from an all-pass characteristic, it was possible to check what influence the spiking activity during the AM part of the stimulus might have exerted on the adaptation status of a neuron (Fig. 8). Figure 8b shows the spike rates of three neurons measured during the SAM stimulus, for each modulation frequency. The BSN1 shown in the left column fired at a rate of ~110 Hz at low modulation frequencies, but its response dropped to <30 Hz for frequencies above 200 Hz. A second BSN1 exhibited a much lower maximal spike rate that dropped to virtually zero at frequencies ≥83 Hz. AN4 showed its typical band stop response described above. In Fig. 8c, the spike rates produced during the control pulse are plotted against modulation frequency of the SAM part (relative to the rate during the adaptation pulse). Most remarkably, the control spike rates showed only little dependence on modulation frequency, and thus on spiking activity during the stimulus' modulation part. If adaptation had depended on the neuron's firing rate during the SAM part, one would have expected an increase of the control pulse spike rate at those frequencies at which the spike rate during the SAM part was so strongly reduced. In other words, even though these neurons nearly ceased to fire at certain modulation frequencies (BSN1 at frequencies >200 Hz and ≥83 Hz, AN4 at 83 and 125 Hz), obviously this massive reduction in firing rate did not lead to a release from adaptation which may have allowed for a recovery of spike rate during the control pulse.

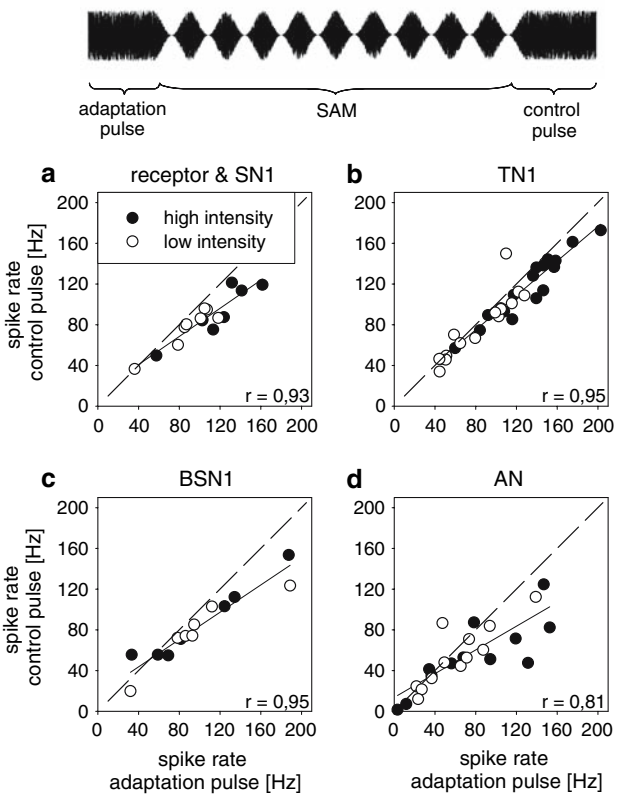


**Fig. 7** Influence of adaptation on spike rates. The spike rate of the first, adaptation pulse is compared to the spike rate found for the control pulse, which followed the SAM part of the stimulus. *Stippled line*: *slope 1*; continuous: regression lines (*r* is indicated in the figures; all correlations highly significant at $P < 0.01$ to 0.001)

## Discussion

The objective of this study was to investigate how changes in signal level would influence the processing of AMs by auditory neurons. If neurons exhibit distinct filter properties for certain temporal features a strong intensity dependence of such filters could lead to a misinterpretation of signals, or at least restrict the useful intensity range. We investigated these questions in the auditory pathway of grasshoppers, since several species use acoustic signals for mate recognition and mate selection, and it is well known that it is the signal's AM pattern that is decisive for the classification of signals (von Helversen and von Helversen 1997, 1998). Hence, the grasshoppers' auditory system

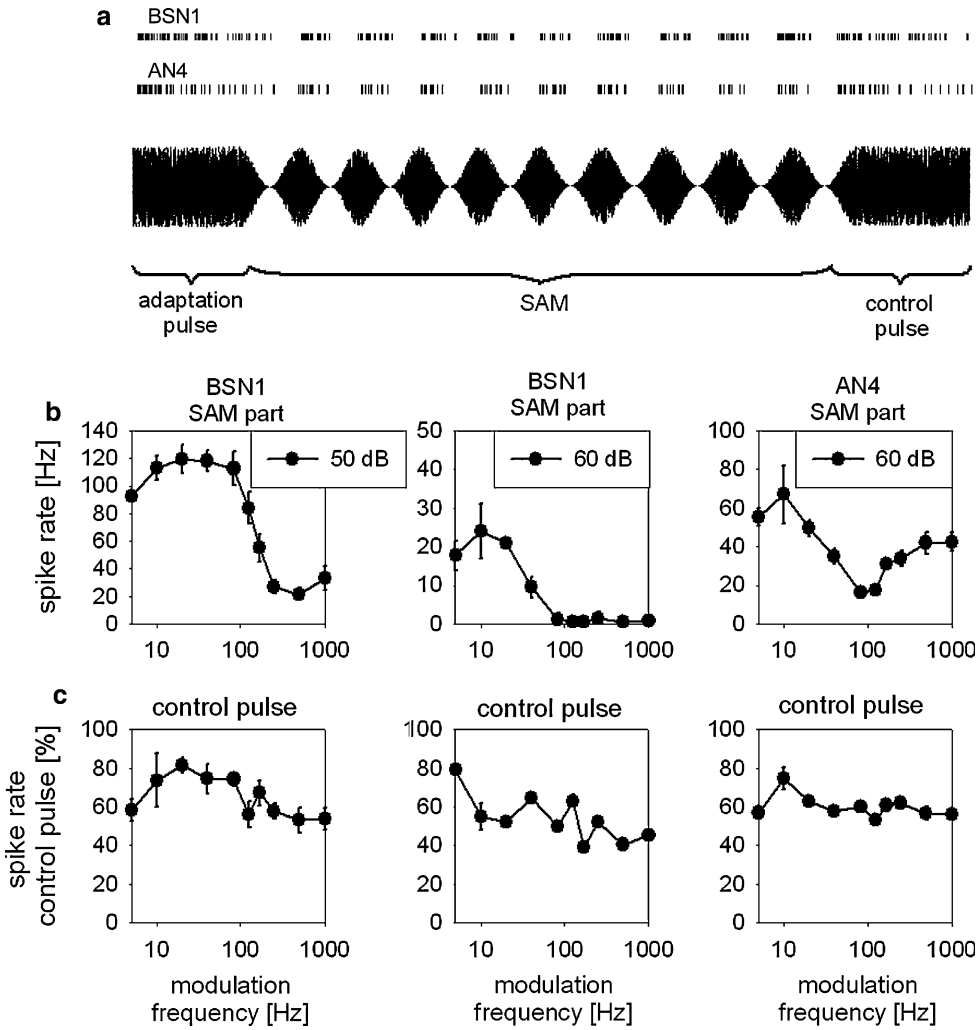


**Fig. 8** Adaptation is independent of the spike rate during the SAM part. **a** Stimulus and two sample spike trains. **b** Spike rates at different SAM frequencies. **c** Normalized spike rate observed for the unmodulated control pulse, at different SAM frequencies. Control pulse spike rates are normalized by the spike rate during the adaptation pulse

must be able to process AM patterns at different time scales. Indeed, in females of the grasshopper *Chorthippus biguttulus* one finds a remarkable capacity to detect tiny gaps, of 2–3 ms duration (von Helversen 1979; von Helversen and von Helversen 1997; Prinz and Ronacher 2002). This ability to resolve gaps, however, depends on intensity—it deteriorates with decreasing SPL (von Helversen 1979)—which was an incentive for the present study.

A major result of this study was the observation that the corner frequencies—i.e. the neurons' upper limits of temporal resolution—did *not* depend on intensity, for most of the neurons investigated (Fig. 3). Only for the primary like TN1 high intensities led to a decrease of the corner frequency. Remarkably, and contrary to expectation, for all neuron types the corner frequencies did also *not* significantly depend on spike rate (Fig. 4). For receptor neurons, this has been reported already (Prinz and Ronacher 2002), but the data presented here suggest that this lack of correlation might be a more general phenomenon. It was unexpected, however, since both inter-spike-interval variability as well as spike count variability (in response to block stimuli) decrease markedly at higher spike rates (Fig. 6 in Vogel et al. 2005), and this change in response variability should have affected the locking of spikes to the signal envelope.

In contrast to the corner frequencies, signal SPL exerted a pronounced influence upon the low-pass or band-pass properties of the tMTF of receptors and local neurons (Fig. 5). This effect, however, is a rather obvious consequence of the increased spike rate. A high SPL of a SAM stimulus acts like an increased duty cycle. Particularly at low AM frequencies high intensities have the effect that a larger proportion of the stimulus period is occupied by spikes, thus reducing the vector strength value (compare Fig. 1, TN1, BSN1; see also Krishna and Semple 2000, for a corresponding result in gerbils). The shift of the BMF with intensity and its dependence on spike rate (Fig. 6), probably have a similar cause. A maximum of vector strength is likely to be found at SAM periods, which trigger just one or two spikes, and thus an increase in spike rate could induce a shift to higher AM frequencies—as indeed was found (Fig. 6a). Such a shift could also explain the independence of the maximum vector strength from

intensity. Notably, both effects, the shift to band-pass and a shift of BMF with intensity, were not observed in ascending neurons. This may have been due to the limited sample size—note that in this class, neurons with different properties have been assembled. However, the generally lower vector strength values found in ascending neurons suggest that the less precise spiking activity, which is typical for this stage of processing, might also have contributed to these differences between ascending and local neurons (Vogel et al. 2005; Vogel and Ronacher 2007; Wohlgemuth and Ronacher 2007);

The results presented here indicate a remarkable intensity invariance of temporal processing, already at the level of local interneurons (see also Benda and Hennig 2007). However, there appears to exist a general division in the AM processing features between receptors and local neurons on the one hand, and the ascending neurons on the other. Ascending neurons exhibited reduced corner frequencies (Fig. 3), no consistent change to band pass behaviour at higher intensities (Fig. 5), and no significant relation between BMF and spike rate (Fig. 6c). These differences point to a change in coding strategy, which appears to take place within the processing network of the metathoracic ganglion: at the level of receptors, and neurons with primary like responses, AMs are coded in the periodicity of neuronal discharges—without any dependence of spike rates on AM frequency. In contrast, in ascending neurons the locking of spikes to the stimulus' envelope becomes less precise, and concomitantly also the corner frequencies are reduced, while at least some of these neurons exhibit rate filter properties. The BSN1 neuron exhibits properties which appear somewhat intermediate between primary like local neurons and ascending neurons (see also Wohlgemuth and Ronacher 2007).

A special case is the AN4 neuron, which has been considered as a potential neuronal correlate for gap detection. In these neurons, an intensity rise triggers a pronounced IPSP, which precedes excitation, and this inhibition is triggered anew after any small gap in the stimulus, thereby suppressing spikes. AN4 shows very similar behaviour in locusts as in *C. biguttulus* (Ronacher and Stumpner 1988), and its response curve, tested with rectangularly modulated stimuli, shows the same characteristic as found in behavioural tests (Ronacher and Stumpner 1988; Stumpner et al. 1991). The results presented in Fig. 2 (middle column) indicate that at low SPL the band stop properties of the rMTF are greatly reduced—which parallels the results of behavioural tests (von Helversen 1979). A comparison with the properties of local neurons, however, suggests that this reduction is a specific property of the AN4 neuron and cannot be accounted for by a reduction of temporal resolution at low intensities in receptors and local neurons (Fig. 3).

A remarkable finding was that the adaptation status of two neurons turned out to be independent of the spike rate during the SAM part of the stimulus (Fig. 8; cf also Benda and Hennig 2007). Spike frequency adaptation is a common feature of neurons in sensory pathways. However, in spite of its universality, a variety of different ionic currents have been found to contribute to this adaptation (for review see Benda and Herz 2003). These currents are triggered by the spiking activity of the neuron, and therefore this type of adaptation has been termed output-driven adaptation (Gollisch and Herz 2004). Gollisch and Herz (2004) provided evidence for "input-driven" adaptation in receptor neurons of locusts, and attributed it to mechanical components. In the examples of Fig. 8, the spike rate observed during the control pulse was not affected by massive changes in spiking activity during the SAM part of the stimulus. Hence, either adaptation occurred in the neuron recorded from but did not depend on its spike rate, or, more likely, the adaptation status was transferred to it from more peripheral neurons—in the case of BSN1 most likely directly by receptor neurons, in AN4 probably via local interneurons.

In general, the steps of processing amplitude modulations found in grasshoppers appear to follow similar lines as in vertebrate hearing systems. Their auditory nerve fibres also exhibit all-pass rMTFs, and spikes are phase locked to the sound envelope. At higher stages of auditory processing, however, the precision of phase-locking is reduced, and tends to be shifted towards rate-based coding schemes (e.g. Rose and Capranica 1985; Rhode and Greenberg 1994; Alder and Rose 2000; Krishna and Semple 2000; Joris et al. 2004). Nevertheless, a high temporal precision at the periphery appears to be essential for the encoding of fast amplitude changes. The apparent transformation in coding strategy and the concomitant reduction of spike timing precision at more central processing levels have been reported from sensory systems as different as the owls' sound localization, bat echolocation, and electrosensation (Konishi 1991; Suga 1988) and may well be a corollary of energy limitation constraints (Laughlin 2001; Schreiber et al. 2002).

**Acknowledgments** We thank Jan Benda, Matthias Hennig, and Jannis Hildebrandt for helpful suggestions on the manuscript, and the DFG for financial support (SFB 618, grant to B.R.). The experiments comply with the current laws on "Principles of animal care" in Germany.

## References

Alder TB, Rose GJ (2000) Integration and recovery processes contribute to the temporal selectivity of neurons in the midbrain of the northern leopard frog, *Rana pipiens*. J Comp Physiol A 186:923–937

Benda J, Hennig RM (2007) Spike-frequency adaptation generates intensity invariance in a primary auditory interneuron. J Comput Neurosci (in press). doi:10.1007/s10827-007-0044-8

Benda J, Herz AVM (2003) A universal model for spike-frequency adaptation. Neural Comput 15:2523–2564

Benda J, Bethge M, Hennig RM, Pawelzik K, Herz AVM (2001) Spike-frequency adaptation: phenomenological model and experimental tests. Neurocomputing 38–40:105–110

Boyan GS (1992) Common synaptic drive to segmentally homologous interneurons in the locust. J Comp Neurol 321:544–554

Feng AS, Hall JC, Siddique S (1991) Neural basis of sound pattern recognition in anurans. Prog Neurobiol 34:313–329

Franz A (2004) Neuronale Variabilität und Korrelationen als begrenzende Faktoren für die Verarbeitung und Kodierung zeitlich strukturierter akustischer Signale. PhD thesis, Humboldt-Universität zu Berlin

Franz A, Ronacher B (2002) Temperature dependence of temporal resolution in an insect nervous system. J Comp Physiol A 188:261–271

Gerhardt HC, Huber F (2002) Acoustic communication in insects and anurans. The University of Chicago Press, Chicago

Gleich O, Klump GM (1995) Temporal modulation transfer functions in the European starling (*Sturnus vulgaris*): 2. Responses of auditory nerve fibers. Hear Res 82:81–92

Gollisch T, Herz AVM (2004) Input-driven components of spike-frequency adaptation can be unmasked in vivo. J Neurosci 25:7435–7444

Grothe B (1994) Interaction of excitation and inhibition in processing of pure tone and amplitude modulated stimuli in the medial superior olive of the mustached bat. J Neurophysiol 71:706–721

Hall JC, Feng AS (1991) Temporal processing in the dorsal medullary nucleus of the northern leopard frog (*Rana pipiens pipiens*). J Neurophysiol 66:955–973

von Helversen D, von Helversen O (1997) Recognition of sex in the acoustic communication of the grasshopper *Chorthippus biguttulus* (Orthoptera, Acrididae). J Comp Physiol A 180:373–386

von Helversen D, von Helversen O (1998) Acoustic pattern recognition in a grasshopper: processing in the frequency or time domain? Biol Cybernet 79:467–476

von Helversen O (1979) Angeborenes Erkennen akustischer Schlüsselreize. Verh Dtsch Zool Ges 72:42–59

Hennig RM, Franz A, Stumpner A (2004) Processing of auditory information in insects. Microsc Res Tech 63:351–374

Joris PX, Schreiner CE, Rees A (2004) Neural processing of amplitude-modulated sounds. Physiol Rev 84:541–577

Konishi M (1991) Similar algorithms in different sensory systems and animals. Cold Spring Harbor Symp Quant Biol 55:575–584

Krahe R, Ronacher B (1993) Long rise times of sound pulses in grasshopper songs improve the directionality cues received by the CNS from the auditory receptors. J Comp Physiol A 173:425–434

Krishna BS, Semple MN (2000) Auditory temporal processing: responses to sinusoidally amplitude-modulated tones in the inferior colliculus. J Neurophysiol 84:255–273

Kroodsma DE, Miller EH (1996) Ecology and evolution of acoustic communication in birds. Cornell University Press, Ithaca

Langner G (1992) Periodicity coding in the auditory system. Hear Res 60:115–142

Laughlin SB (2001) Energy as a constraint on the coding and processing of sensory information. Curr Opin Neurobiol 11:475–480

Machens CK, Stemmler MB, Prinz P, Krahe R, Ronacher B, Herz AVM (2001) Representation of acoustic communication signals by insect auditory receptor neurons. J Neurosci 21:3215–3227

Michelsen A (1985) Time resolution in auditory systems. Springer, New York

Pearson KG, Robertson RM (1981) Interneurons co-activating hindleg flexor and extensor moto-neurons in the locust. J Comp Physiol A 144:391–400

Prinz P, Ronacher B (2002) Temporal modulation transfer functions in auditory receptor fibres of the locust (*Locusta migratoria*). J Comp Physiol A 188:577–587

Rhode WS, Greenberg S (1994) Encoding of amplitude modulation in the cochlear nucleus of the cat. J Neurophysiol 71:1797–1825

Rokem A, Watzl S, Gollisch T, Stemmler MB, Herz AVM, Samengo I (2006) Spike-timing precision underlies the coding efficiency of auditory receptor neurons. J Neurophysiol 95:2541–2552

Römer H (1976) Die Informationsverarbeitung tympanaler Rezeptorelemente von *Locusta migratoria* (Acrididae, Orthoptera). J Comp Physiol 109:101–122

Römer H, Marquart V (1984) Morphology and physiology of auditory interneurons in the metathoracic ganglion of the locust. J Comp Physiol A 155:249–262

Ronacher B, von Helversen D, von Helversen O (1986) Routes and stations in the processing of auditory directional information in the CNS of a grasshopper, as revealed by surgical experiments. J Comp Physiol A 158:363–374

Ronacher B, Stumpner A (1988) Filtering of behaviourally relevant parameters of a grasshopper's song by an auditory interneuron. J Comp Physiol A 163:517–523

Rose GJ, Capranica RR (1985) Sensitivity to amplitude modulated sounds in the anuran auditory nervous system. J Neurophysiol 53:446–465

Sachs L (1999). Angewandte Statistik: Anwendung statistischer Methoden. Springer, Berlin

Schreiber S, Machens CK, Herz AVM, Laughlin SB (2002). Energy-efficient coding with discrete stochastic elements. Neural Comput 14:1323–1346

Stumpner A (1988) Auditorische thorakale Interneurone von *Chorthippus biguttulus* L.: Morphologische und physiologische Charakterisierung und Darstellung ihrer Filtereigenschaften für verhaltensrelevante Lautattrappen. PhD thesis, Friedrich-Alexander Universität Erlangen

Stumpner A, von Helversen D (2001) Evolution and function of auditory systems in insects. Naturwissenschaften 88:159–170

Stumpner A, Ronacher B (1991) Auditory interneurons in the metathoracic ganglion of the grasshopper *Chorthippus biguttulus*: 1. Morphological and physiological characterization. J Exp Biol 158:391–410

Stumpner A, Ronacher B, von Helversen O (1991) Auditory interneurons in the metathoracic ganglion of the grasshopper *Chorthippus biguttulus*: 2. Processing of temporal patterns of the song of the male. J Exp Biol 158:411–430

Suga N (1988) What does single-unit analysis in the auditory cortex tell us about information processing in the auditory system. In: Rakic P, Singer W (eds) Neurobiology of neocortex. Wiley, New York, pp 331–349

Vogel A, Hennig RM, Ronacher B (2005) Increase of neuronal response variability at higher processing levels as revealed by simultaneous recordings. J Neurophysiol 93:3548–3559

Vogel A, Ronacher B (2007) Neural correlations increase between consecutive processing levels in the auditory system of locusts. J Neurophysiol 97:3376–3385

Wohlgemuth S, Neuhofer D, Ronacher B (2007) Comparing the neuronal encoding in two not closely related grasshopper species: what differs is different? In: Proceedings of the 31st Göttingen Neurobiology Conference

Wohlgemuth S, Ronacher B (2007) Auditory discrimination of amplitude modulations based on metric distances of spike trains. J Neurophysiol 97:3082–3092